Video Article

Gold Nanorod-assisted Optical Stimulation of Neuronal Cells

Chiara Paviolo[1], Sally L. McArthur[1], Paul R. Stoddart[1]

[1]Biotactical Engineering, Faculty of Science, Engineering and Technology, Swinburne University of Technology

Correspondence to: Chiara Paviolo at cpaviolo@swin.edu.au

URL: https://www.jove.com/video/52566
DOI: doi:10.3791/52566

Keywords: Neuroscience, Issue 98, gold nanorods, external absorber, neural stimulation, laser excitation, optical stimulation, neuronal cells, *in vitro* models.

Date Published: 4/27/2015

Citation: Paviolo, C., McArthur, S.L., Stoddart, P.R. Gold Nanorod-assisted Optical Stimulation of Neuronal Cells. *J. Vis. Exp.* (98), e52566, doi:10.3791/52566 (2015).

Abstract

Recent studies have demonstrated that nerves can be stimulated in a variety of ways by the transient heating associated with the absorption of infrared light by water in neuronal tissue. This technique holds great potential for replacing or complementing standard stimulation techniques, due to the potential for increased localization of the stimulus and minimization of mechanical contact with the tissue. However, optical approaches are limited by the inability of visible light to penetrate deep into tissues. Moreover, thermal modelling suggests that cumulative heating effects might be potentially hazardous when multiple stimulus sites or high laser repetition rates are used. The protocol outlined below describes an enhanced approach to the infrared stimulation of neuronal cells. The underlying mechanism is based on the transient heating associated with the optical absorption of gold nanorods, which can cause triggering of neuronal cell differentiation and increased levels of intracellular calcium activity. These results demonstrate that nanoparticle absorbers can enhance and/or replace the process of infrared neural stimulation based on water absorption, with potential for future applications in neural prostheses and cell therapies.

Video Link

The video component of this article can be found at https://www.jove.com/video/52566/

Introduction

Recent studies have demonstrated that the transient heating associated with the absorption of infrared light by water (wavelength >1,400 nm) can be used to induce action potentials in nerve tissue[1] and intracellular calcium transients in cardiomyocytes[2]. The use of infrared light has raised great interest for applications in neural prostheses, due to the potential finer spatial resolution, lack of direct contact with the tissue, minimization of stimulation artifacts, and removal of the need to genetically modify the cells prior to stimulation (as required in optogenetics)[1]. Despite all of these benefits, recently developed thermal models suggested that the target tissue/cells may be affected by cumulative heating effects, when multiple stimulus sites and/or high repetition rates are used[3,4].

In response to these challenges, researchers have recognized the potential to use extrinsic absorbers for nerve stimulation to produce more localized heating effects in the tissue. Huang *et al.* demonstrated this principle by using superparamagnetic ferrite nanoparticles to remotely activate the temperature-sensitive TRPV1 channels in HEK 293 cells with a radio-frequency magnetic field[5]. Although this technique may allow for deeper penetration (magnetic fields interact relatively weakly with tissue), the responses were only recorded over periods of seconds, rather than the millisecond durations required in bionic devices[5]. Similarly, Farah *et al.* demonstrated electrical stimulation of rat cortical neurons with black micro-particles *in vitro*. They showed cell-level precision in stimulation using pulse durations on the order of hundreds of μs and energies in the range of μJ, potentially allowing for faster repetition rates[6].

The use of extrinsic absorbers has also been applied to induce morphological changes *in vitro*. Ciofani *et al.* showed a ~40% increase in neuronal cell outgrowth using piezoelectric boron nitride nanotubes excited by ultrasound[7]. Similarly, endocytosed iron oxide nanoparticles in PC12 cells have been reported to enhance neurite differentiation in a dose-dependent manner, due to the activation of cell adhesion molecules with the iron oxide[8].

Recently, the interest in extrinsic absorbers to assist neural stimulation has also focused on the use of gold nanoparticles (Au NPs). Au NPs have the ability to efficiently absorb laser light at the plasmonic peak and to dissipate it into the surrounding environment in the form of heat[9]. Amongst all of the available particle shapes, the optical absorption of gold nanorods (Au NRs) conveniently matches the therapeutic window of biological tissues (near infrared - NIR, wavelength between 750-1,400 nm)[10]. Moreover, in the context of neural stimulation, the use of Au NRs provides relatively favorable biocompatibility and a wide range of surface functionalization options[11]. Recent studies have shown that a stimulatory effect on differentiation can be induced after continuous laser exposures of Au NRs in NG108-15 neuronal cells[12]. Similarly, intracellular calcium transients were recorded in neuronal cells cultured with Au NRs after laser irradiation modulated with variable frequencies and pulse lengths[13]. Cell membrane depolarization was also recorded after NIR laser illumination of Au NRs in primary cultures of spiral ganglion neurons[14]. The first *in vivo* application with irradiated Au NRs has been demonstrated just recently. Eom and coworkers exposed Au NRs at their plasmonic peak and

recorded a six-fold increase in the amplitude of compound nerve action potentials (CNAPs) and a three-fold decrease in the stimulation threshold in rat sciatic nerves. The enhanced response was attributed to local heating effects resulting from the excitation of the NR plasmonic peak[15].

In the present paper, protocols for investigating the effects of laser stimulation in NG108-15 neuronal cells cultured with Au NRs are specified. These methods provide a simple, yet powerful, way to irradiate cell populations *in vitro* using standard biological techniques and materials. The protocol is based on a fiber-coupled laser diode (LD) that allows safe operation and repeatable alignment. The Au NR sample preparation and laser irradiation methods can be further extended to different particle shapes and neuronal cell cultures, providing that the specific synthesis and culture protocols are known, respectively.

Protocol

1. Au NRs Preparation

Note: Au NRs can be synthesized by a number of recipes[16], or purchased from commercial vendors.

1. Measure the initial optical density (OD) of the Au NR solution via UV-Vis spectroscopy, by recording the absorption values from 300 nm to 1,000 nm with a resolution of 0.5-2 nm. Vary the volume of the solution to be used with the available cuvette.
2. Evaluate the initial NP molar concentration with a suitable technique[17] (*e.g.* UV-Vis spectroscopy, single particle inductively coupled plasma mass spectrometry, transmission electron microscopy) or use the concentration values provided by the vendor.
3. Prepare a 5 ml stock solution by diluting the initial Au NR sample to reach an OD = 1. For the best repeatability, keep the OD constant for all of the tested samples. Follow the commercial vendor's protocol for the composition of the diluting solvent. If unsure, use deionized water.
4. Centrifuge 1 ml of the Au NR solution twice for 15 min at 7,800 x g to remove any chemical excess from the solution. Centrifugation cycles can vary in force and time (*e.g.* 20 min at 5,600 × g)[18].
5. Remove the supernatants and re-suspend the NRs in deionized water. As re-suspended particles might form aggregates in solution, prepare them daily to have the best results. Alternatively, store in a fridge for no longer than 1 week. Do not freeze.
6. Before using under cell culture conditions, sonicate the Au NR solution for 5 min and then sterilize with UV light for 30 min (UV radiation intensity not less than 400 $mW \cdot m^{-2}$ at 254 nm).

2. NG108-15 Neuronal Cell Line Culture and Differentiation

1. For the cell culture medium, prepare 500 ml of sterile Dulbecco's modified Eagle medium (DMEM) containing 10% (w/v) fetal calf serum (FCS), 1% (w/v) L-glutamine, 1% (w/v) penicillin/streptomycin and 0.5% (w/v) amphotericin B.
   Note: Supplements can be aliquoted, stored at -20 °C and added to the media on the day required. Cell culture medium can be refrigerated in a sterile condition for a maximum of 1 month.
2. For the cell differentiation medium, prepare 50 ml of sterile DMEM containing 1% (w/v) L-glutamine, 1% (w/v) penicillin/streptomycin and 0.5% (w/v) amphotericin B.
3. Grow NG108-15 neuronal cells in 10 ml of cell culture medium in T75 flasks made of polystyrene in an incubator with humidified atmosphere (5% CO_2 at 37 °C). Normally, seed 1.5-2 × 10^5 cells in each flask to be ready in 3-4 days. Change cell culture medium every two days.
   Note: To prevent genetic drifts or variation, do not use cells older than passage 21 for experiments.
4. When 70-80% confluent in culture, change the medium with warm fresh cell culture medium. Mechanically detach the cells by gently knocking the bottom of the confluent flask. Do not use trypsin.
5. Centrifuge the cell suspension for 5 min at 600 x g and re-suspend the cell pellet in 2 ml of warm cell differentiation medium.
6. Seed 2 × 10^4 $cells/cm^2$ in a tissue culture polystyrene 96 well plate with 200 µl of cell differentiation medium. Incubate the experiment for 1 day at 5% CO_2/37 °C.
7. Add between 3.2 × 10^9-4.2 ×1 0^{10} particles/ml of Au NR solution on day 2 and incubate it for additional 24 hr. Do not add the particles for the control experiments.
   Note: As an alternative control, Au NPs with a well-differentiated peak absorption wavelength can be used for comparison purposes[14]. For a more consistent cell behavior, keep the cell density constant and do not modify the well surface prior to cell seeding.

3. Neurite Outgrowth Enhancement

1. Couple the laser with a single mode optical fiber (numerical aperture = 0.13) and terminate it with a fiber connector (FC connectors are convenient and commonly available). Measure the output laser power with a standard power meter. To obtain the most effective results, match the peak wavelength of the laser to the plasmon resonance peak of the NRs.
2. On day 3 following NR incubation, fix the FC connector to the well. Irradiate samples and controls at RT for 1 min in continuous wave, for different laser powers. Allow the culture to proceed for 3 additional days at 5% CO_2/37 °C. Repeat the laser irradiation for a minimum of 3 independent measurements.
   Note: Different irradiation times and pulse frequencies may be selected, depending on the application.
3. Characterize the laser in terms of beam diameter and laser irradiance ($W \cdot cm^{-2}$).
   1. For a standard single mode fiber, use $NA = n \cdot \sin\theta$, where n is the refractive index of the medium in use and θ is the half-angle of the cone of light exiting the fiber (see **Figure 1A**). From trigonometry, $r = \tan\theta \cdot d$, where r is the beam radius and d is the distance between the fiber and the sample. The FC connector matches the diameter of the well, therefore illuminating the sample at a distance d = 2.70 ± 0.20 mm. Light exits the fiber in water (n = 1.33), giving $r = \tan(\sin\text{-}1(NA/n)) \cdot d$.
   2. Using the latter equation, calculate the laser beam radius, the corresponding beam area and the average laser irradiance (laser power divided by beam area) at the target (see the example graph in **Figure 1B**). These values represent the average irradiance over the illuminated area.
   3. Evaluate the errors for the measurements with the general theory of error propagation.

Note: The distance between the FC connector and the sample can be measured by photographs of the experimental arrangement and post-processing of the image using appropriate software (*e.g.* ImageJ).

4. At day 5, remove cell differentiation medium from the experiments and fix the samples with 3.7% (v/v) formaldehyde solution for 10 min, then permeabilize the cells with 0.1% (v/v) Triton X-100 for 20 min.
5. Add 3% (w/v) bovine serum albumin (BSA) to the samples for 60 min to block the unreacted protein binding sites. Label the samples for anti-βIII-tubulin overnight (5 µg/ml in PBS supplemented with 1% of BSA) at 4 °C.
6. Incubate the cells for 90 min in the dark with an appropriate secondary antibody (*e.g.* TRITC-conjugated anti-mouse IgG antibody) using a concentration of 0.4-2 µg/ml in 1% BSA in PBS. Label the cell nuclei with DAPI (0.1 µg/ml in de-ionized water) for 10 min.
Note: Antibody conjugation and concentration might vary according to the company protocol. Wash samples with PBS twice for 5 min after each staining stage.

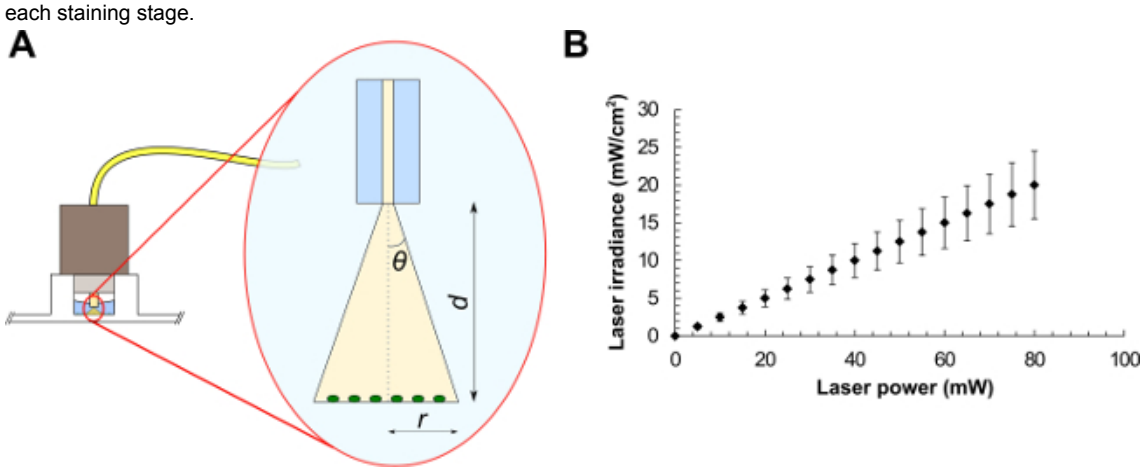

7. Image samples by epifluorescence or confocal microscopy using at least a 20× objective. Choose the microscope filters accordingly to the secondary antibody. Select a DAPI filter (λ_{EX} = 358 nm; λ_{EM} = 488 nm) to visualize the cell nuclei.
8. Analyze the pictures by assessing: i) the maximum neurite length (record the length from the tip of the neurite to the beginning of the cell body), ii) the number of neurites per neuronal cell (sum up all of the neurites per cell) and iii) the percentage of cells with neurites (divide the total number of cells expressing βIII-tubulin by the total number of cells with a positively stained nucleus)[19].

4. Laser-induced Intracellular Ca^{2+} Imaging

1. Prepare a 20% (w/v) stock solution of Pluronic F-127 by dissolving 2 g of solute in 10 ml of anhydrous dimethyl sulfoxide (DMSO). Heat the solution of Pluronic F-127 at 40 °C for about 20 min to increase the solubility. Prepare it in advance if stored at RT.
2. On day 3 following NR incubation, prepare a balanced salt solution (BSS; 135 mM NaCl, 4.5 mM KCl, 1.5 mM $CaCl_2$, 0.5 mM $MgCl_2$, 5.6 mM glucose, and 10 mM HEPES, pH 7.4) and supplemented it with 5 µM of Fluo-4 AM in DMSO and 0.1% (w/v) of Pluronic F-127 solution.
Note: BSS solution can be prepared in advance and refrigerated for a maximum of 1 month. Add the supplements (Fluo-4 AM and Pluronic F-127) on the day of the experiment.
3. Remove cell differentiation medium and replace it with the supplemented BSS solution. To obtain the best results with an inverted confocal microscope, incubate the cells in a micro-slide well.
4. Load NG108-15 cells with Fluo-4 AM for 30 min in the dark at 5% CO_2/37 °C. Following the incubation time, wash samples twice with BSS to remove any extracellular unloaded fluorophore.
5. Couple the laser with a single mode optical fiber and cleave the tip using standard techniques. Observe the resulting tip under an optical microscope, to ensure a high-quality surface (*i.e.* the tip should be perpendicular to the fiber axis and flat upon microscopy inspection).
    1. Measure the output laser power with a standard power meter. Insert the light delivery fiber into an optical fiber holder and affix it to a micropositioner. Refer to Brown *et al.*[20] for more details on optical fiber preparation and positioning.
    Caution: Follow the general rules for laser safety during the measurement of the laser power (*e.g.* do not look directly into laser beam, wear laser safety goggles during handling, prevent stray light exposure to other lab users).

6. Connect an oscilloscope to the portable laser to monitor the optical modulation. Use a binary signal with variable frequencies (0.5-2 Hz) and pulse lengths (20-100 msec). Connect the laser using the modulation signal as transistor-transistor logic (TTL) input for the microscope, following the setup shown in Paviolo *et al.*[13].
    1. Place the cells under an inverted confocal microscope and position the light delivery fiber 250 ± 50 µm away from the target cell in transmission illumination mode. At this distance, use the equations presented in 3.3.1 to calculate the beam radius at the target.

7. Use an argon-ion laser (488 nm) to excite the internalized Fluo-4 AM dye (λ_{EX} = 494 nm; λ_{EM} = 516 nm) and the synchronized LD for the excitation of the endocytosed NRs. Perform the imaging at RT of samples and controls using at least a 40× objective by collecting time-series scans with 256 × 256 pixels/frame resolution in roundtrip mode with a frequency of at least 4 Hz. Perform a recording without any LD excitation to identify any argon-ion laser interference (baseline noise).
8. Remove the background from the data using adaptively weighted penalized least-squares algorithms[21]. Plot the induced Ca^{2+} variations as a function of time. Analyze the transient peaks in the fluorescence intensity using image post-processing software by thresholding at a level three times the standard deviation of the baseline noise (3σ).

Representative Results

By using Protocols 1, 2, and 3 described here, a stimulatory effect on differentiation was observed in NG108-15 neuronal cells cultured with Au NPs (Au NRs, poly(styrenesulfonate)-coated Au NRs and silica-coated Au NRs) after laser exposures between 1.25 and 7.5 $W \cdot cm^{-2}$. Confocal images of rhodamineB-labelled Au NRs demonstrated that the particles were internalized from day 1 of incubation[12]. The localization was predominantly observed in the cell cytoplasm, indicating that the preferred mechanism of uptake was via the cell body membrane[12]. The main morphological changes detected after inducing differentiation in NG108-15 neuronal cells were the arrest of proliferation, the expression of βIII-tubulin protein and the outgrowth of neurites, which were analyzed in terms of maximum length and number[22].

Samples cultured with NRs showed a neurite length increase at the laser irradiance levels measured here (between 1.25 and 7.5 $W \cdot cm^{-2}$). Control samples (cells cultured without NPs and irradiated with the same laser power) showed no significant change in length. Using an irradiation dose of 7.5 $W \cdot cm^{-2}$, the final neurite length of NG108-15 cultured with Au NRs was roughly 36% higher ($p < 0.01$) than the non-laser-irradiated samples. This behavior was not specifically linked to the surface chemistry of the NRs. These values were almost 20% greater than the neurites developed by NG108 -15 alone and exposed to the same value of laser exposure ($p < 0.05$)[12]. These results are in line with previously published studies on PC12 neuronal cells cultured with piezoelectric nanotubes and irradiated with ultrasound radiation[7].

Control experiments without Au NRs also showed some stimulatory effects of the 780 nm light in terms of percentage of neurons with neurites and number of neurites per neuron. This stimulation was more effective at lower laser powers (1.25 $W \cdot cm^{-2}$) with a subsequent decrease at the highest laser energy (7.5 $W \cdot cm^{-2}$)[12]. A moderate stimulation caused by the NPs without any laser irradiation (poly(styrenesulfonate)-coated and silica-coated only) was detected in the percentage of neurons with neurites[12]. These results are in line with recently published observations that gold nanoparticles can increase neuronal activity *in vitro*[23,24]. **Figure 2** shows an example of epifluorescence images of differentiated NG108-15 neuronal cells cultured alone (**Figure 2A**) or with Au NRs (**Figure 2B**) and irradiated with different laser powers (indicated in the figure).

The potential for photo-generated intracellular Ca^{2+} release was assessed using pulsed NIR light in accordance with Protocols 1, 2, and 4. Calcium ions play an important role in different cellular activities, such as mitosis, muscle contraction and neurite extension[25,26]. In response to a stimulus, Ca^{2+} increases, oscillates and decreases, leading to the activation, modulation or termination of a specific cell function. Recently, Ca^{2+} transients have also been observed as a consequence of IR laser exposure in cardiomyocytes. In that work, the Ca^{2+} responses evoked after IR exposure exhibited lower amplitudes and faster recovery times than the spontaneous Ca^{2+} transients[2]. **Figure 3** shows an example of NG108-15 neuronal cells loaded with Fluo-4 AM and imaged with a confocal microscope. Fluo-4 AM was observed to enter the cell membrane in a non-disruptive manner, resulting in a generally uniform distribution of the indicator across the cell cytoplasm. Only minor nuclear or cytoplasmic organelle staining was detected. As previously indicated, NRs were expected to be located intracellularly[12]. NG108-15 neuronal cells alone or cultured with Au NRs and poly(styrenesulfonate)-coated-Au NRs were exposed thereafter to laser irradiances between 0.07 $J \cdot cm^{-2}$ and 370 $J \cdot cm^{-2}$, with the laser frequency modulated in the range of 0.5-2 Hz.

Figure 4 shows representative examples of how the amplitude of the responses was mapped as a function of time. The amplitude of the Ca^{2+} response varied with the radiant exposure (**Figure 4A**-**C**) and was observed not to be consistently triggered by the laser pulses (**Figure 4C**)[13]. The most likely explanations were the transient depletion of intracellular Ca^{2+} stores attributed to incomplete Ca^{2+} loading[2] or the different efficiency of NR internalization in the neuronal cells. When NRs were not used in culture (control experiments, **Figure 4D**), a stimulatory effect of the 780 nm light was also observed. However, this produced lower fluorescence amplitude peaks and lower probability of activation (detected in only 16% of the analyzed samples). Overall, a 48% probability of NR laser-induced cell activation was achieved and despite the background events due to the 780 nm light, exposure of NR-treated cells demonstrated higher stimulation efficiency with lower laser energy and higher peaks of response[13]. In fact, the calcium response was found to peak at 0.33 $J \cdot cm^{-2}$ in the NR-treated cells. This was attributed to thermal inhibition[13]. During the experiments, no evidence of blebbing or any other form of cell membrane disruption was detected, which is consistent with the results of Huang *et al.* that reported cellular photodestruction with a relatively high power density of 19 $W \cdot cm^{-2}$ applied for 4 min[27]. No spontaneous activity in the NR-treated cells was recorded without laser exposure.

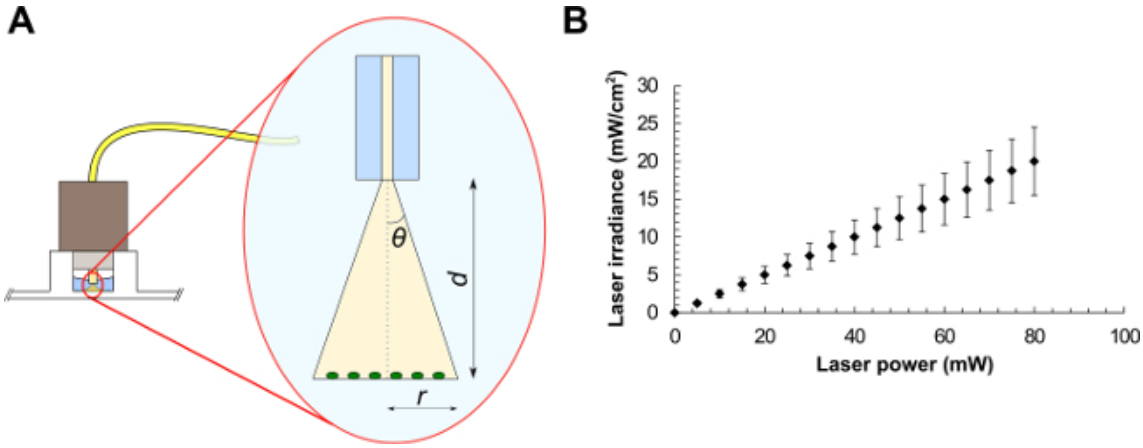

Figure 1: Optical fiber experimental setup (**A**) and average laser irradiances as a function of the laser power for a laser beam of area equals to 0.4 mm^2 (**B**). Beam parameters are (**A**): the half-angle of the maximum cone of light exiting the fiber (θ), the beam radius (r) and the distance between the optical fiber and the sample (d).

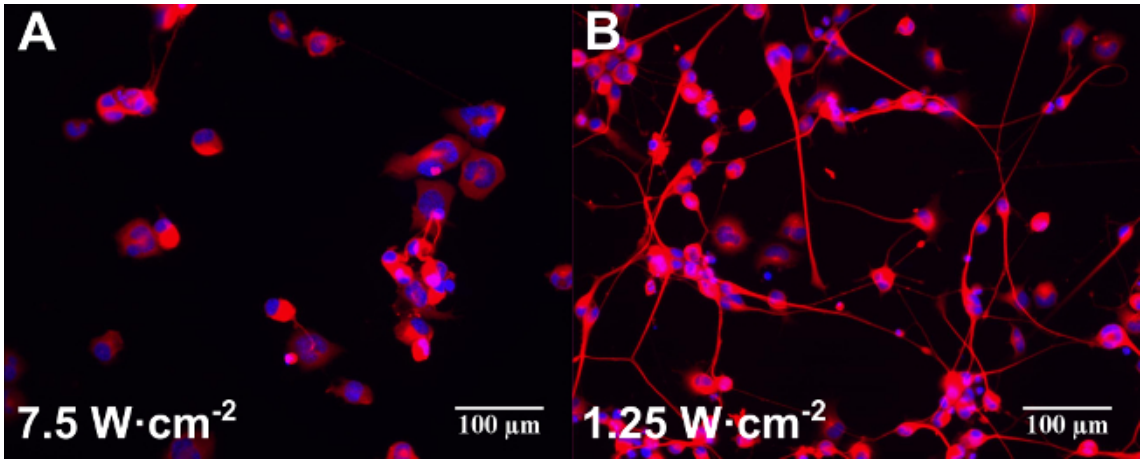

Figure 2: Examples of epifluorescence images of differentiated NG108-15 neuronal cells cultured alone (**A**) or with Au NRs (**B**) and irradiated with different laser powers (indicated in the figure). Samples were incubated for one day before laser irradiation. Cells were fixed and labeled for anti-β-III tubulin (red) and DAPI (blue) three days after laser irradiation. Scale bars are 100 µm.

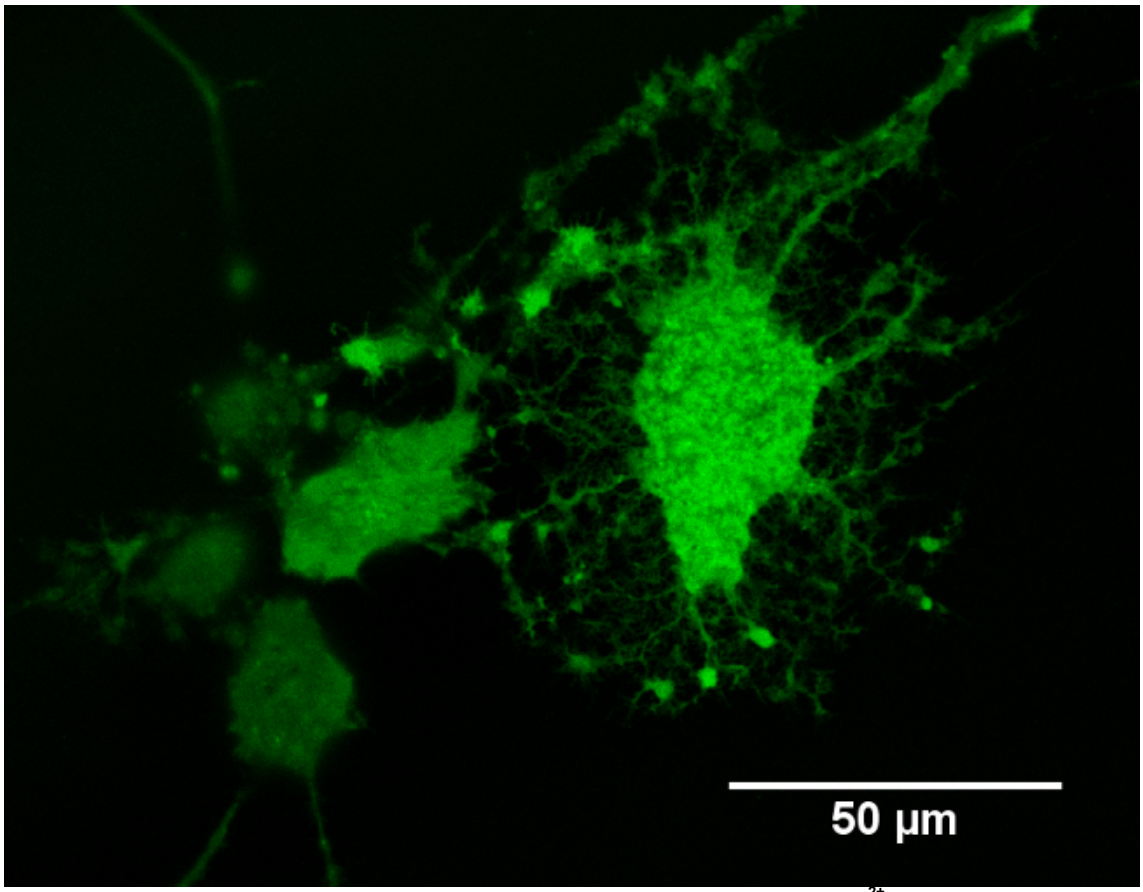

Figure 3: Example of differentiated NG108-15 neuronal cells loaded with Fluo4-AM Ca^{2+} indicator. The image was taken using an inverted confocal microscope with a 40X oil-immersion objective.

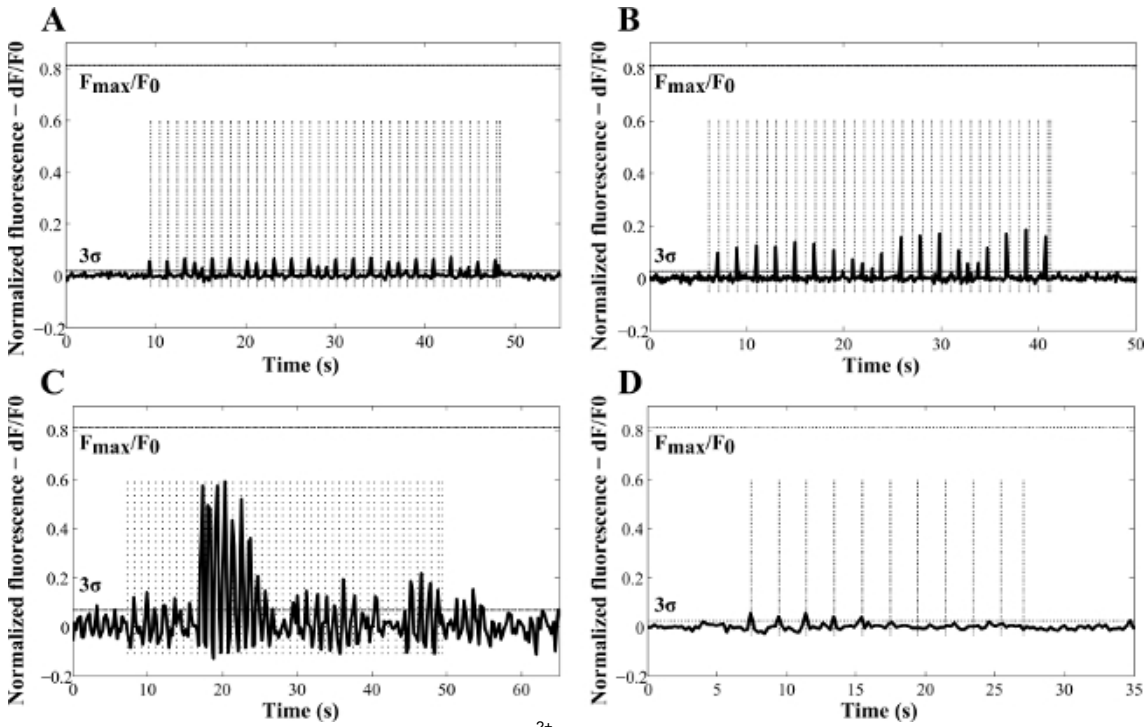

Figure 4: Representative examples of laser-induced Ca^{2+} variations as a function of time in NG108-15 neuronal cells cultured in serum-free conditions for three days with (**A**) poly(styrenesulfonate)-Au NRs, (**B**, **C**) Au NRs, and (**D**) without NRs (control sample). These results were obtained with laser pulses of 100 msec (**A**, **C**, **D**) and 50 msec (**B**). The frequencies used for the experiments (dashed vertical lines) were 1 Hz (**A**-**C**) and 0.5 Hz (**D**). The calculated radiant exposures were 69.4 J·cm^{-2} (**A**), 34.7 J·cm^{-2} (**B**), 0.37 J·cm^{-2} (**C**) and 138.87 J·cm^{-2} (**D**). F_{max}/F_0 indicates the maximum fluorescence increase detected in NG108 -15 neuronal cells, from calibration with ionomycin (reproduced with permission[13]).

Discussion

The protocols outlined in this presentation describe how to culture, differentiate and optically stimulate neuronal cells using extrinsic absorbers. The NR characteristics (*e.g.* dimensions, shape, plasmon resonance wavelength and surface chemistry) and the laser stimulation parameters (such as wavelength, pulse length, repetition rate, *etc.*) can be varied to match different experimental needs. The effects on cell behavior can be monitored using standard biological assays and materials. Overall the approach provides a simple, yet powerful, way to irradiate cell populations *in vitro* and could be extended to primary cells, tissue samples and *in vivo* studies.

The main requirements that Au NRs need to satisfy to be used for biological applications are stability (both chemical and physical) and biocompatibility. The latter is particularly critical, due to the presence of a cationic surfactant (commonly CTAB) on the surface of the Au. CTAB is known to induce cytotoxicity both *in vitro*[28] and *in vivo*[29] and it is commonly used during the synthesis process to drive the NR-shape formation[30]. Stability and biocompatibility are often improved by depositing additional coatings on the Au NR surface (*e.g.* polyethylene glycol, silica)[31]. To assess the biocompatibility, different assays can be used *in vitro* (*e.g.* live/dead, MTS, MTT, etc.) while histological analysis is often performed during tissue experiments[7,8,12,15].

Another challenge to face when working with nanomaterials is the difficulty of correctly determining their molar concentration. The huge variety of NPs in terms of shape, size, and chemical properties makes the techniques currently available suitable for only certain classes of particles. For example, the standard dynamic light scattering method assumes that NPs have a spherical shape and scatter light isotropically[17]. Therefore, application of this method to Au NRs results in discrepancies between the measured concentration and the real one. The issue of NP concentration is particularly problematic if related to the nanomedicine field, where the concentration administered needs to be precisely controlled in order to maximize the efficacy of the process (*e.g.* for drug delivery applications) and minimize the toxicity of the nanomaterials[17]. In the studies reported here, the optical density used gave good results in terms of cell viability and particle number.

Due to their intrinsic absorption properties, Au NPs are often used in combination with a laser source. During the exposure, absorption and scattering are the two main processes likely to occur at the surface of the NPs. If the laser wavelength matches the plasmon resonance wavelength, absorption often prevails over scattering, exciting the conduction electrons at the NP surface. These form an electron gas that moves away from its equilibrium position and creates a resonant coherent oscillation called the localized surface plasmon resonance (LSPR). The energy is then transferred to the NP crystal lattice as heat, which is thereafter dissipated rapidly into the surrounding environment[32]. Since heat is the main effect observed after the excitation of the NR LSPR, it is advisable to monitor cell viability after laser exposure.

It has been hypothesized that the observed effects on the neurite outgrowth and the intracellular Ca^{2+} pathway were due to the transient heating arising from excitation of the LSPR. This hypothesis is in line with the activation of the temperature-sensitive TRPV1 channel after magnetic exposure of ferrite NPs[5]. This process is also consistent with observations that thermally sensitive TRPV4 channels play an important role in infrared nerve stimulation[33]. At a molecular level, it has been recently shown that TRPV4 is thermosensitive only after the interaction of

phosphoinositide -4,5 -biphosphate (PIP_2) with the channel[34]. Therefore, it is possible that the transient heating arising after NR excitation could serve to accelerate and/or induce the opening of the TRPV4 channels. This hypothesis can be confirmed by future Ca^{2+} experiments by using Ca^{2+}- free medium and/or molecular controls over the PIP_2 depletion.

Different groups have also demonstrated that small temperature gradients over the physiological temperature range can be used to induce other responses, such as neuronal growth cone guiding[25] or depolarizing currents in human embryonic kidney cells[35]. Yong and coworkers recorded a significant increase in electrical signal activity in primary auditory neurons cultured with silica-coated Au NRs after laser irradiation of the NRs at the LSPR. The heating produced by the laser-irradiated particles was measured using patch-clamp techniques[14]. More recently, Eom *et al.* recorded an increase in the amplitude of CNAPs after laser exposure of 3.4×10^9 Au NRs when continuously perfused in the vicinity of the sheath of the nerve bundle of a rat sciatic nerve[15].

The stimulatory effect of the 780 nm laser diode observed during the experiments was not linked to heat generated by water absorption, as this is known to be negligible at 780 nm[36]. Previously published results have also reported stimulatory effects of 780 nm light on neuronal tissue *in vivo*[37,38]. *In vitro* studies have demonstrated the involvement of reactive oxygen species in the process[39]. However, the detailed mechanisms by which NIR stimulation affects gene transcription and other cellular activities are currently unresolved. Current data suggests the interplay of different effects in the stimulation, including photon absorption within chromophores in the mitochondria (almost 50% of the energy at 780 nm might be absorbed by cytochrome *c* oxidase)[37,39-41], changes in membrane permeability to calcium[37] and inhibition of inflammatory activity in the cells[37].

The results presented in this manuscript demonstrate that nanoparticle absorbers hold great promise for future applications in optical stimulation of neuronal cells. The main advantage lies in the ability of NIR light to penetrate deep into tissues (therapeutic window). These results also show that nanoparticle absorbers can enhance and/or replace the process of infrared neural stimulation based on water absorption. For future applications in neural prostheses, it would be of interest to investigate different surface functionalizations with chemical affinity for neuronal axons, which are the main targets for many optical stimulation applications.

Disclosures

The authors have no competing interests to disclose.

Acknowledgements

The authors would like to acknowledge NanoVentures Australia for travel funding support and Prof. John Haycock for having partially hosted this research at the University of Sheffield and Ms. Jaimee Mayne for her help during the filming.

References

1. Richter, C. P., Matic, A. I., Wells, J. D., Jansen, E. D., Walsh, J. T. Neural stimulation with optical radiation. *Laser. Photonics Rev.* **5**, (1), 68-80 (2011).
2. Dittami, G. M., Rajguru, S. M., Lasher, R. A., Hitchcock, R. W., Rabbitt, R. D. Intracellular calcium transients evoked by pulsed infrared radiation in neonatal cardiomyocytes. *J. Physiol.* **589**, (6), 1295-1306 (2011).
3. Thompson, A. C., Wade, S. A., Brown, W. G. A., Stoddart, P. R. Modeling of light absorption in tissue during infrared neural stimulation. *J. Biomed. Opt.* **17**, (7), 075002-075002 (2012).
4. Thompson, A. C., Wade, S. A., Cadusch, P. J., Brown, W. G., Stoddart, P. R. Modeling of the temporal effects of heating during infrared neural stimulation. *J. Biomed. Opt.* **18**, (3), 035004 (2013).
5. Huang, H., Delikanli, S., Zeng, H., Ferkey, D. M., Pralle, A. Remote control of ion channels and neurons through magnetic-field heating of nanoparticles. *Nat. Nanotechnol.* **5**, (8), 602-606 (2010).
6. Farah, N., *et al.* Holographically patterned activation using photo-absorber induced neural-thermal stimulation. *J. Neural. Eng.* **10**, (5), (2013).
7. Ciofani, G., *et al.* Enhancement of neurite outgrowth in neuronal-like cells following boron nitride nanotube-mediated stimulation. *ACS Nano.* **4**, (10), 6267-6277 (2010).
8. Kim, J. A., *et al.* Enhancement of neurite outgrowth in PC12 cells by iron oxide nanoparticles. *Biomaterials.* **32**, (11), 2871-2877 (2011).
9. Myroshnychenko, V., *et al.* Modelling the optical response of gold nanoparticles. *Chem. Soc. Rev.* **37**, (9), 1792-1805 (2008).
10. Choi, W. I., Sahu, A., Kim, Y. H., Tae, G. Photothermal cancer therapy and imaging based on gold nanorods. *Ann. Biomed. Eng.* **40**, (2), 534-546 (2011).
11. Zhan, Q., Qian, J., Li, X., He, S. A study of mesoporous silica-encapsulated gold nanorods as enhanced light scattering probes for cancer cell imaging. *Nanotechnology.* **21**, (5), 055704 (2010).
12. Paviolo, C., *et al.* Laser exposure of gold nanorods can increase neuronal cell outgrowth. *Biotechnol. Bioeng.* **110**, (8), 2277-2291 (2013).
13. Paviolo, C., Haycock, J. W., Cadusch, P. J., McArthur, S. L., Stoddart, P. R. Laser exposure of gold nanorods can induce intracellular calcium transients. *J. Biophotonics.* **7**, (10), 761-765 (2014).
14. Yong, J., *et al.* Gold-nanorod-assisted near-infrared stimulation of primary auditory neurons. *Adv. Healthcare Mater.* (2014).
15. Eom, K., *et al.* Enhanced infrared neural stimulation using localized surface plasmon resonance of gold nanorods. *Small.* (2014).
16. Juste, J., Pastoriza-Santos, I., Liz-Marzán, L. M., Mulvaney, P. Gold nanorods: Synthesis, characterization and applications. *Coordination Chemistry Reviews.* (17-18), 1870-1901 (2005).
17. Shang, J., Gao, X. Nanoparticle counting: towards accurate determination of the molar concentration. *Chem. Soc. Rev.* **43**, (21), 7267-7278 (2014).
18. Sharma, V., Park, K., Srinivasarao, M. Shape separation of gold nanorods using centrifugation. *Proc. Natl. Acad. Sci.* **106**, (13), 4981-4985 (2009).

19. Kaewkhaw, R., Scutt, A. M., Haycock, J. W. Anatomical site influences the differentiation of adipose-derived stem cells for schwann-cell phenotype and function. *Glia.* **59**, (5), 734-749 (2011).
20. Brown, W. G. A., Needham, K., Nayagam, B. A., Stoddart, P. R. Whole cell patch clamp for investigating the mechanisms of infrared neural stimulation. *JoVE.* (77), (2013).
21. Cadusch, P. J., Hlaing, M. M., Wade, S. A., McArthur, S. L., Stoddart, P. R. Improved methods for fluorescence background subtraction from Raman spectra. *J. Raman Spectrosc.* **44**, (11), 1587-1595 (2013).
22. Daud, M. F. B., Pawar, K. C., Claeyssens, F., Ryan, A. J., Haycock, J. W. An aligned 3D neuronal-glial co-culture model for peripheral nerve studies. *Biomaterials.* **33**, (25), 5901-5913 (2012).
23. Jung, S., *et al.* Intracellular gold nanoparticles increase neuronal excitability and aggravate seizure activity in the mouse brain. *PLoS ONE.* **9**, (3), e91360 (2014).
24. Salinas, K., Kereselidze, Z., DeLuna, F., Peralta, X., Santamaria, F. Transient extracellular application of gold nanostars increases hippocampal neuronal activity. *J. Nanobiotechnology.* **12**, (1), 31 (2014).
25. Ebbesen, C. L., Bruus, H. Analysis of laser-induced heating in optical neuronal guidance. *J. Neurosci. Meth.* **209**, (1), 168-177 (2012).
26. Iwanaga, S., *et al.* Location-dependent photogeneration of calcium waves in HeLa cells. *Cell Biochem. Biophys.* **45**, (2), 167-176 (2006).
27. Huang, X., Jain, P. K., El-Sayed, I. H., El-Sayed, M. A. Determination of the minimum temperature required for selective photothermal destruction of cancer cells with the use of immunotargeted gold nanoparticles. *Photochem. Photobiol.* **82**, (2), 412-417 (2006).
28. Connor, E. E., Mwamuka, J., Gole, A., Murphy, C. J., Wyatt, M. D. Gold nanoparticles are taken up by human cells but do not cause acute cytotoxicity. *Small.* **1**, (3), 325-327 (2005).
29. Isomaa, B., Reuter, J., Djupsund, B. M. The subacute and chronic toxicity of cetyltrimethylammonium bromide (CTAB), a cationic surfactant, in the rat. *Arch. Toxicol.* **35**, (2), 91-96 (1976).
30. Juste, J., Pastoriza-Santos, I., Liz-Marzán, L., Mulvaney, P. Gold nanorods: synthesis, characterization and applications. *Coord. Chem. Rev.* **249**, (17-18), 1870-1901 (2005).
31. Dreaden, E. C., Alkilany, A. M., Huang, X., Murphy, C. J., El-Sayed, M. A. The golden age: gold nanoparticles for biomedicine. *Chem. Soc. Rev.* **41**, (7), 2740-2779 (2012).
32. Huang, X., Jain, P. K., El-Sayed, I. H., El-Sayed, M. A. Plasmonic photothermal therapy (PPTT) using gold nanoparticles. *Lasers Med. Sci.* **23**, (3), 217-228 (2008).
33. Albert, E. S., *et al.* TRPV4 channels mediate the infrared laser-evoked response in sensory neurons. *J. Neurophysiol.* **107**, (12), 3227-3234 (2012).
34. Garcia-Elias, A., *et al.* Phosphatidylinositol-4,5-biphosphate-dependent rearrangement of TRPV4 cytosolic tails enables channel activation by physiological stimuli. *Proceedings of the National Academy of Sciences of the United States of America.* **110**, (23), 9553-9558 (2013).
35. Shapiro, M. G., Homma, K., Villarreal, S., Richter, C. -P., Bezanilla, F. Infrared light excites cells by changing their electrical capacitance. *Nat. Commun.* **3**, (736), (2012).
36. Roggan, A., Friebel, M., Dörschel, K., Hahn, A., Müller, G. Optical properties of circulating human blood in the wavelength range 400-2500 nm. *J. Biomed. Opt.* **4**, (1), 36-46 (1999).
37. Byrnes, K. R., *et al.* Light promotes regeneration and functional recovery and alters the immune response after spinal cord injury. *Lasers Surg. Med.* **36**, (3), 171-185 (2005).
38. Wu, X., *et al.* 810 nm wavelength light: an effective therapy for transected or contused rat spinal cord. *Lasers Surg. Med.* **41**, (1), 36-41 (2009).
39. Grossman, N., Schneid, N., Reuveni, H., Halevy, S., Lubart, R. 780 nm low power diode laser irradiation stimulates proliferation of keratinocyte cultures: involvement of reactive oxygen species. *Lasers Surg. Med.* **22**, (4), 212-218 (1998).
40. Wong-Riley, M. T. T., *et al.* Photobiomodulation directly benefits primary neurons functionally inactivated by toxins - Role of cytochrome c oxidase. *J. Biol. Chem.* **280**, (6), 4761-4771 (2005).
41. Beauvoit, B., Kitai, T., Chance, B. Contribution of the mitochondrial compartment to the optical properties pf the rat liver: a theoretical and practical approach. *Biophys. J.* **67**, (6), 2501-2510 (1994).

